Single-View Echocardiographic Analysis for Left Ventricular Outflow Tract Obstruction Prediction in Hypertrophic Cardiomyopathy: A Deep Learning Approach

Jiesuck Park, MD, Jiyeon Kim, MS, Jaeik Jeon, MSc, Yeonyee E. Yoon, MD, PhD, Yeonggul Jang, PhD, Hyunseok Jeong, BS, Seung-Ah Lee, MD, PhD, Hong-Mi Choi, MD, In-Chang Hwang, MD, Goo-Yeong Cho, MD, PhD, and Hyuk-Jae Chang, MD, PhD, *Seongnam, Gyeonggi, and Seoul, Republic of Korea*

Background: Accurate left ventricular outflow tract obstruction (LVOTO) assessment is crucial for hypertrophic cardiomyopathy (HCM) management and prognosis. Traditional methods, requiring multiple views, Doppler, and provocation, is often infeasible, especially where resources are limited. This study aimed to develop and validate a deep learning (DL) model capable of predicting severe LVOTO in HCM patients using only the parasternal long-axis (PLAX) view from transthoracic echocardiography (TTE).

Methods: A DL model was trained on PLAX videos extracted from TTE examinations (developmental dataset, *n* = 1,007) to capture both morphological and dynamic motion features, generating a DL index for LVOTO (DLi-LVOTO; range 0-100). Performance was evaluated in an internal test dataset (ITDS; *n* = 87) and externally validated in the distinct hospital dataset (DHDS; *n* = 1,334) and the LVOTO reduction treatment dataset (*n* = 156).

Results: The model achieved high accuracy in detecting severe LVOTO (pressure gradient 50 mm Hg), with area under the receiver operating characteristics curve of 0.97 (95% CI, 0.92-1.00) in ITDS and 0.93 (0.92-0.95) in DHDS. At a DLi-LVOTO threshold of 70, the model demonstrated a specificity of 97.3% and negative predictive value of 96.1% in ITDS. In DHDS, a cutoff of 60 yielded a specificity of 94.6% and negative predictive value of 95.5%. The DLi-LVOTO also decreased significantly after surgical myectomy or Mavacamten treatment, correlating with reductions in peak pressure gradient ($P < .001$ for all).

Conclusions: Our DL-based approach predicts severe LVOTO using only the PLAX view from TTE, serving as a complementary tool when Doppler assessment is unavailable and for monitoring treatment response. (J Am Soc Echocardiogr 2025;38:1115-26.)

Keywords: Hypertrophic cardiomyopathy, Deep learning, Echocardiography, Left ventricular outflow tract obstruction, Prediction

From the Cardiovascular Center and Division of Cardiology, Department of Internal Medicine, Seoul National University Bundang Hospital, Seongnam, Gyeonggi (J.P., Y.E.Y., H.-M.C., I.-C.H., G.-Y.C.); Department of Internal Medicine, Seoul National University College of Medicine, Seoul, Republic of Korea (J.P., Y.E.Y., H.-M.C., I.-C.H., G.-Y.C.); Ontact Health, Seoul, Republic of Korea (J.K., J.J., Y.E.Y., Y.J., S.-A.L., H.-J.C.); CONNECT-AI Research Center, Yonsei University College of Medicine, Seoul, Republic of Korea (H.J., S.-A.L., H.-J.C.); Department of Internal Medicine, Graduate School of Medical Science, Brain Korea 21 Project, Yonsei University College of Medicine, Seoul, Republic of Korea (H.J.); and Division of Cardiology, Severance Cardiovascular Hospital, Yonsei University College of Medicine, Yonsei University Health System, Seoul, Republic of Korea (H.-J.C.).

Drs. Park and Kim contributed equally to this work.

This work was supported by a grant from the Institute of Information and Communications Technology Planning and Evaluation (IITP) funded by the Ministry of Science and ICT (MSIT), Korea (grant no. 2022000972, Development of a Flexible Mobile Healthcare Software Platform Using 5G MEC). It was also supported by the Medical AI Clinic Program through the National IT Industry Promotion Agency (NIPA) funded by the MSIT (grant no. H0904-24-1002).

Reprint requests: Yeonyee E. Yoon, MD, PhD, Professor, Division of Cardiology, Cardiovascular Center, Seoul National University Bundang Hospital, 82, 173 Beon-gil, Gumi-ro, Bundang-gu, Seongnam-si, Gyeonggi-do, Republic of Korea (E-mail: *yeonyeeyoon@snubh.org*).

0894-7317

https://doi.org/10.1016/j.echo.2025.08.008

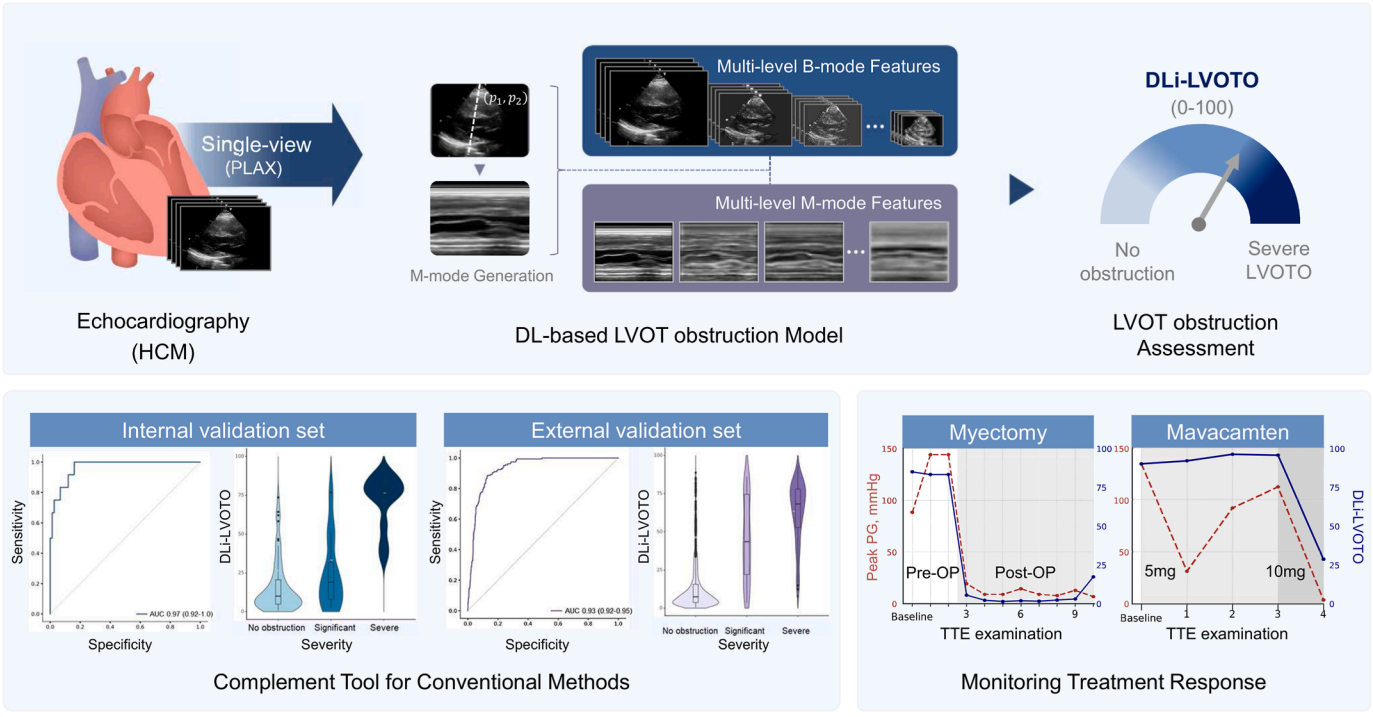

Central Illustration Deep learning–based single-view echocardiographic analysis for LVOTO in HCM.

INTRODUCTION

Hypertrophic cardiomyopathy (HCM) is one of the most common genetic cardiomyopathies, with an estimated prevalence of 1 in 200 to 1 in 500.[1] The phenotype of HCM is highly heterogeneous, ranging from asymptomatic presentation to severe outcomes such as sudden cardiac death. Among the various factors influencing symptoms and prognosis, left ventricular outflow tract (LVOT) obstruction (LVOTO) plays a pivotal role.[1,2] When LVOTO becomes severe, it not only contributes to symptoms such as exertional dyspnea, chest pain, and syncope but also serves as the key determinant in guiding clinical management, including pharmacological treatment, septal reduction intervention, or surgery.[2] Therefore, accurate identification of LVOTO is critical in the clinical evaluation of HCM patients.

See page 1127 in issue for related content.

Transthoracic echocardiography (TTE) is the primary imaging modality for diagnosing and evaluating HCM.[2] Left ventricular outflow tract obstruction is typically assessed through TTE using Doppler imaging and multiple echocardiographic views, often incorporating provocation maneuvers.[2] However, these assessments require substantial expertise in image acquisition and interpretation, are time-intensive, and are subject to technical variability, interobserver variability, and patient cooperation. These limitations can hinder their feasibility, especially in acute care settings using handheld devices, in resource-limited community hospitals, or in patients unable to tolerate provocation. Among TTE views, the parasternal long-axis (PLAX) view is one of the most fundamental, offering critical insights into cardiac anatomy and dynamic function. Therefore, leveraging this single, widely available view for automated prediction of LVOTO could improve accessibility and maintain clinical accuracy, even in settings where expert evaluation is limited or advanced Doppler-equipped systems are unavailable.

Recent advancements in deep learning (DL) have demonstrated significant potential in automating and enhancing medical image interpretation, and TTE is no exception. Deep learning algorithms can identify complex patterns in imaging data that may elude human observers, thereby improving diagnostic accuracy and efficiency. For instance, efforts have been made to accurately assess conditions such as aortic stenosis (AS) and diastolic dysfunction using limited two-dimensional (2D) TTE images, even without Doppler input.[3-7] Despite these advances, the application of DL for predicting LVOTO using single-view TTE in HCM patients remains underexplored. A recent attempt utilized the apical 4-chamber (A4C) view to predict LVOTO through a DL-based model.[8] However, this single-view approach is fundamentally limited by the A4C's indirect visualization of the LVOT, resulting in suboptimal performance that may restrict its clinical applicability.

In the present study, we aimed to develop a hybrid spatiotemporal network that learns directly from resting 2D PLAX TTE videos, which provide a clear visualization of the LVOT, to predict the presence of severe LVOTO in HCM patients without the need for Doppler input or provocation maneuvers. To achieve this, our framework integrates global B-mode spatial context with multiresolution M-mode features, enabling the construction of a comprehensive spatiotemporal representation of LVOTO dynamics. Specifically, we designed a novel, fully automated multislice M-mode generation framework derived directly from PLAX 2D video data, eliminating the need for manual placement or predefined anatomical landmarks. This multislice M-mode approach dynamically tracks key anatomical structures throughout the cardiac cycle, capturing subtle hemodynamic cues that are often only observed during provocation maneuvers. Our model's ability to synchronize

Abbreviations

2D = Two-dimensional

A4C = Apical 4-chamber

AI = Artificial intelligence

AS = Aortic stenosis

CE = Cross-entropy

DDS = Developmental Dataset

DHDS = Distinct hospital dataset

DL = Deep learning

DLi-LVOTO = Deep learning index for left ventricular outflow tract obstruction

Grad-CAM = Gradient-Weighted Class Activation Mapping

HCM = Hypertrophic cardiomyopathy

IQ = Image quality

ITDS = Internal test dataset

LV = Left ventricle

LVOT = Left ventricular outflow tract

LVOTO = Left ventricular outflow tract obstruction

MV = Mitral valve

NPV = Negative predictive value

PG = Pressure gradient

PLAX = Parasternal long-axis

PPV = Positive predictive value

SAM = Systolic anterior motion

TTE = Transthoracic echocardiography

spatial and temporal information allows for the detection of flow abnormalities and structural changes in real time, enhancing both interpretability and diagnostic precision. This study presents the development and validation of our DL-based model and evaluates its predictive performance for severe LVOTO. Additionally, we assess its potential as a practical complementary tool to conventional Doppler-based assessments, which often require multiple TTE views with provocation maneuvers, offering a streamlined method for LVOTO detection, particularly valuable in resource-limited settings and for less experienced operators.

METHODS

Study Population and Data Sources

The DL-based model presented in this study was developed and validated using the Open AI Dataset Project (AI-Hub) dataset, an initiative supported by the South Korean government's Ministry of Science and Information and Communication Technology.[5,6,9-13] This dataset comprised 30,000 echocardiographic examinations retrospectively collected from 5 tertiary hospitals between 2012 and 2021, encompassing a wide range of cardiovascular diseases, including HCM. From this dataset, we identified cases categorized as HCM and applied the following inclusion criteria: (1) availability of echocardiographic reports, (2) a clinical diagnosis of HCM established by identifying a maximal end-diastolic wall thickness ≥15 mm in any segment of the left ventricle (LV), with other potential causes of hypertrophy excluded, and (3) TTE, in which the presence or absence of LVOTO had been assessed by Doppler-based pressure gradient (PG) measurements. While Doppler data were necessary to establish ground truth for LVOTO classification, they were not used as model input. Furthermore, no examinations were excluded based on image quality (IQ), as we aimed to capture typical variations observed in real-world clinical TTE images.

To develop the DL-based LVOTO prediction algorithm, we created the Developmental Dataset (DDS), consisting of 722 patients with 1,007 TTE examinations, which were divided into training, validation, and test datasets in an 8:1:1 ratio, comprising 578, 71, and 73 patients (809, 111, and 87 TTE examinations, respectively), ensuring that no patient overlap occurred among these subsets. Transthoracic echocardiography data from Severance Hospital were excluded from the DDS and designated as the Distinct Hospital Dataset (DHDS) for independent external tests. The DHDS included 573 patients with 1,334 TTE examinations, serving as an external dataset to evaluate model generalizability. Both the DDS and DHDS explicitly excluded any TTE data from patients who had undergone LVOT gradient reduction treatments, including surgical myectomy or Mavacamten therapy, to avoid potential confounding effects during model development and validation. Additionally, we collected pre- and posttreatment TTE data from obstructive HCM patients who underwent LVOT gradient reduction treatment at Seoul National University Bundang Hospital and Severance Hospital. This dataset comprises 17 patients with 112 TTE examinations from those who underwent surgical myectomy and 13 patients with 44 TTE examinations from those treated with Mavacamten. To eliminate any risk of data leakage, these patients were entirely excluded from the DDS, regardless of when their TTE examinations were performed. A schematic overview of the dataset composition and allocation is provided in Supplemental Methods 1.

The study protocol was approved by the institutional review boards of all participating institutions, with a waiver of informed consent granted due to the retrospective study design. All clinical data were fully anonymized prior to analysis. The study was conducted in accordance with the principles outlined in the Declaration of Helsinki (2013).

TTE Acquisition and Interpretation

All TTE studies were conducted by trained echocardiographers or cardiologists and interpreted by board-certified cardiologists specializing in echocardiography as part of routine clinical care. All TTE examinations included in this study were standard TTEs; exercise or pharmacological stress tests were not included. However, provocation maneuvers that can be performed during standard TTE, such as the Valsalva maneuver, were included to evaluate LVOTO. For the assessment of LVOTO, continuous-wave Doppler was used in the apical 3-chamber or 5-chamber view to measure the LVOT peak velocity (V_{max}, m/sec). The Bernoulli equation ($PG = 4 \times V_{max}^2$) was then applied to calculate the LVOT peak PG. If a Valsalva maneuver successfully induced or exacerbated LVOTO, the peak PG measured during Valsalva was used for classification. Conversely, if the Valsalva maneuver did not lead to any measurable increase in LVOTO, the resting PG was used instead. Left ventricular outflow tract obstruction was classified based on the LVOT peak PG: a peak PG ≥ 30 mm Hg was defined as significant LVOTO, and a peak PG ≥ 50 mm Hg was defined as severe LVOTO.[2,14] Importantly, the ground truth labels used for model training and evaluation were based solely on Doppler-assessed LVOT gradient; cases of midventricular or apical obstruction were not included as positive labels.

As part of image interpretation, the HCM phenotype was classified based on morphological characteristics observed on TTE to support subgroup analyses. Patients were categorized into 4 phenotypes: apical, septal, diffuse, mixed, and others. Detailed definitions of these phenotypes are provided in Supplemental Methods 2.

Model Development

We developed a novel DL model to predict severe LVOTO using single-view, 2D PLAX TTE videos acquired at rest, eliminating the need for Doppler assessments. The model was trained to infer the presence of severe LVOTO as determined by Doppler assessment. It was explicitly designed to capture both morphological (i.e., spatial) and motion (M-mode) features critical for LVOTO assessment (Figure 1).

HIGHLIGHTS

- A DL model predicts severe LVOTO from resting PLAX view.
- No Doppler or provocation maneuvers are required for DL-based LVOTO assessment.
- DLi-LVOTO enables risk stratification of LVOTO.
- DLi-LVOTO supports response monitoring of LVOT gradient reduction treatment.
- DLi-LVOTO provides complementary tools in the management of HCM patients.

Our network architecture employs a modified R(2 + 1)D-18 backbone,[15] based on a ResNet-18[16] using factorized three-dimensional convolutions (2D spatial + one-dimensional temporal) to retain full temporal resolution for video data. To effectively capture the motion dynamics critical for predicting severe LVOTO, we introduced an automated M-mode generation process that leverages a spatial transformer network.[17] The model autonomously learns and predicts an optimal M-mode line and extracts the motion information along that line in a fully differentiable manner. An auxiliary mean squared error loss constrains the M-mode trajectory to pass through the mitral valve (MV) tip, ensuring alignment with clinically relevant anatomical landmarks. This approach mimics the conventional clinician-derived M-mode acquisition from the PLAX view, where the M-mode line is typically placed to evaluate LVOT dynamics effectively. Additionally, we implemented multilevel M-mode generation at various network depths, fusing these representations to create comprehensive motion embeddings. The generated M-mode representations were independently processed using a pretrained EfficientNet-B3[10,18] M-mode, and spatiotemporal (B-mode) features were then fused via concatenation.

The model was trained using a supervised learning approach with a primary classification task to distinguish severe and nonsevere LVOTO, optimized using a binary cross-entropy (CE) loss. Since severe LVOTO is defined based on peak PG, which can be augmented by provocation, but PLAX videos used in this study were recorded at rest, we introduced an auxiliary regression task to predict the LVOT PG measured at rest. This guided the network to learn subtle hemodynamic features from resting images that correlate with LVOTO severity, allowing it to infer additional predictive cues beyond rest-

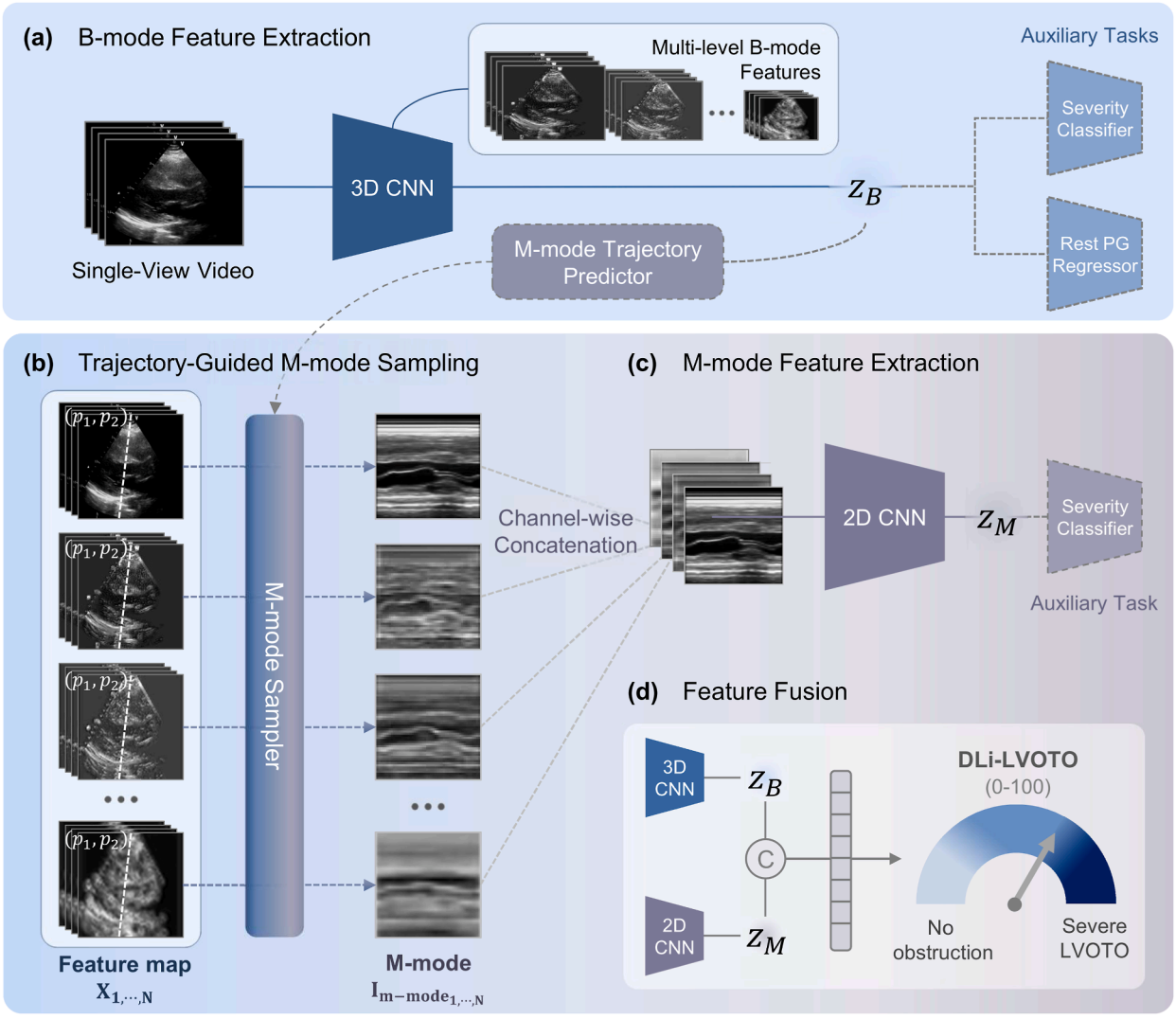

Figure 1 Deep learning framework for LVOTO assessment. **(A)** B-mode feature extraction, **(B)** trajectory-guided M-mode sampling, **(C)** M-mode feature extraction, **(D)** feature fusion. *CNN*, Convolutional neural network.

only inputs for a diagnosis that often requires provocation. Additionally, an early exit strategy with auxiliary classifiers attached to intermediate features improved gradient flow and training stability. Overall, the training objective was formulated as a summation of 3 loss components: binary CE loss for classification, mean absolute error loss for PG regression, and anatomical mean squared error loss to ensure physiologically meaningful feature extraction. All loss terms were equally weighted (1.0). All PLAX videos were first normalized to 24 fps and then resized to 224 × 224 pixels. To assess the effect of frame rate variability on model performance, we additionally tested the trained model across different normalized frame rates (10-45 fps); results confirmed stable performance above 20 fps (Supplemental Method 3). To enhance generalization and robustness of the model, we applied random augmentations including noise injection, sector masking, haze, depth-dependent attenuation, dynamic gain variation, brightness/contrast adjustment, temporal noise, sharpening, and geometric transforms such as translation, rotation, and cropping.[19]

For patient-level DL index of LVOTO (DLi-LVOTO; range, 0-100), multiple PLAX videos from a single patient were individually analyzed, and their DLi-LVOTO scores were averaged. Additional details on the model architecture, M-mode processing, and training parameters are available in Supplemental Methods 4. Further analyses on the incremental contributions of key components, including auxiliary regression loss, anatomical alignment loss, early-exit strategy, and multilevel M-mode generation, are presented in Supplemental Methods 5. The model represents the latest advancement in our artificial intelligence (AI)-driven HCM evaluation module (USfeat_HCM.ai, Ontact Health), which integrates validated features such as view classification and automatic measurement capabilities.[10,12,13,20]

Model Validation and Statistical Analysis

The performance of our DL-based LVOTO prediction model was validated using an internal test dataset (ITDS) and an independent external dataset (DHDS). Additionally, we assessed the model's performance in serial TTE examinations of patients who underwent LVOT gradient reduction therapy, including surgical myectomy and Mavacamten treatment.

The DL-based prediction algorithm's performance for severe LVOTO in the ITDS and DHDS was evaluated using receiver operating characteristics curve analysis, with the area under the curve and 95% CI as key performance measures. We also visualized the distribution of the DLi-LVOTO across categories of no or insignificant LVOTO, significant LVOTO, and severe LVOTO using violin plots. Additionally, we stratified DLi-LVOTO into 10-unit intervals and evaluated its diagnostic performance at each cutoff, assessing key performance metrics, including accuracy, F1-score, sensitivity, specificity, positive predictive value (PPV), and negative predictive value (NPV).

To further assess model robustness, subgroup analyses were performed based on HCM phenotypes and PLAX IQ. Hypertrophic cardiomyopathy was categorized into 3 phenotypes—septal, diffuse/mixed, and apical subtypes—based on morphological characteristics observed during TTE. In addition, PLAX IQ was classified into 3 levels: excellent (clear visualization of key structures with sharp endocardial borders), good (minor shadowing or dropout with adequate diagnostic quality), and fair (partial obscuration due to artifacts or suboptimal window, yet still interpretable).[21]

Saliency maps were generated using the Gradient-Weighted Class Activation Mapping (Grad-CAM),[22] with representative maps presented for each severity level to highlight the areas with the greatest influence on the model's prediction. In patients who were treated with surgical myectomy or Mavacamten, we compared baseline and follow-up TTE studies performed before and after treatment by visualizing changes in LVOT peak PG and DLi-LVOTO.

RESULTS

Baseline Clinical and Echocardiographic Characteristics

Baseline clinical and echocardiographic characteristics across datasets are shown in Table 1. The median age of patients was 65 years (interquartile range, 54-74) in the DDS and 60 years (interquartile range, 50-70) in the DHDS, with similar male predominance (66.3% and 67.0%, respectively). The DDS exhibited a relatively balanced distribution of HCM phenotypes: apical (38.4%), septal (30.7%), and diffuse or mixed (28.9%). In contrast, the DHDS was predominantly composed of the septal type (71.4%). The overall prevalence of LVOTO was 28.9% in DDS and 15.4% in DHDS. Additionally, when comparing the Mavacamten treatment dataset and the surgical myectomy dataset, patients who received Mavacamten were generally older and had a higher diffuse or mixed-type prevalence. In contrast, those who underwent surgical myectomy were relatively younger, with a predominance of the septal type.

To further characterize the population, Table 2 provides a stratified comparison of baseline characteristics according to the presence and severity of LVOTO. Across both DDS and DHDS, patients with severe LVOTO tended to have smaller LV end-diastolic dimensions and greater septal wall thickness compared to those without LVOTO. However, there was considerable overlap in other variables such as age, left ventricular ejection fraction, and left atrial volume index.

Performance of DL-Based Prediction of LVOTO

Our DL-based LVOTO prediction model was able to reliably detect the presence of severe LVOTO using single-view, 2D PLAX videos, achieving an area under the receiver operating characteristics curve of 0.97 (95% CI, 0.92-1.00) in ITDS and 0.93 (95% CI, 0.92-0.95) in DHDS (Figure 2). Subgroup analysis based on HCM phenotypes, including septal, diffuse/mixed, and apical subtypes, demonstrated that the model's performance remained consistently robust across all subtypes in both ITDS and DHDS validations (Supplemental Result 1). Furthermore, IQ subgroup analysis revealed that model performance remained stable regardless of PLAX view quality. Even in good and fair IQ subgroups, the area under the receiver operating characteristics curve values were comparable to those in the excellent group, indicating the model's robustness against variations in IQ (Supplemental Result 2). The DLi-LVOTO distribution showed a gradual increase with LVOTO severity in both ITDS and DHDS, reflecting a consistent relationship between the predicted scores and clinical classification (Figure 2). Additionally, in a subgroup of patients with small LV end-systolic dimensions (<20 mm), the DLi-LVOTO score remained significantly higher in those with LVOTO than in those without, suggesting that the model does not simply reflect cavity size (Supplemental Result 3).

Table 3 presents the diagnostic performance of DLi-LVOTO across different cutoff values for identifying severe LVOTO in both the ITDS and DHDS. In the ITDS, a cutoff of 70 yielded the highest accuracy (94.3%) with a specificity of 97.3% and NPV of 96.1%. The same cutoff also demonstrated high specificity (96.4%) in the DHDS, suggesting its potential utility when the goal is to rule in LVOTO and prioritize further evaluation confidently. Conversely, a cutoff of 30 provided 100.0% sensitivity in the ITDS and 93.0% in the DHDS, with corresponding high NPVs (100.0% and 98.8%, respectively), supporting its use as a conservative threshold for ruling out severe obstruction.

Table 1 Baseline characteristics

		DDS			External test dataset		
	Overall DDS	Training dataset	Validation dataset	Internal test dataset (ITDS)	DHDS (DHDS)	Surgical myectomy dataset	Mavacamten treatment dataset
Demographics							
No. of patients	722	578	71	73	573	17	13
Age, years	65 (54-74)	65 (55-74)	60 (51-72)	65 (56-75)	60 (50-70)	60 (46-65)	69 (51-77)
Gender, male	479 (66.3)	385 (66.6)	55 (77.5)	39 (53.4)	384 (67.0)	9 (52.9)	6 (46.2)
HCM type							
Apical	277 (38.4)	226 (39.1)	24 (33.8)	27 (37.0)	114 (19.9)	0 (0.0)	0 (0.0)
Septal	222 (30.7)	178 (30.8)	24 (33.8)	20 (27.4)	409 (71.4)	10 (58.8)	3 (23.1)
Diffuse or mixed	209 (28.9)	161 (27.9)	23 (32.4)	25 (34.2)	40 (7.0)	7 (41.2)	9 (69.2)
Others	14 (1.9)	13 (2.2)	0 (0.0)	1 (1.4)	10 (1.7)	0 (0.0)	1 (7.7)
Echocardiographic data							
No. of TTEs	1,005	809	111	87	1,334	112	44
LVEDD, mm	45 (41-49)	45 (41-48)	45 (42-48)	46 (42-50)	47 (44-51)	44 (40-49)	42 (37-46)
IVS, mm	15 (12-18)	15 (12-18)	16 (14-18)	14 (12-18)	18 (16-20)	17 (15-20)	18 (14-22)
LVEF, %	65 (61-69)	65 (61-69)	65 (61-69)	65 (62-69)	68 (62-73)	65 (58-69)	67 (62-69)
LAVI, mL/m^2	46 (37-58)	45 (36-58)	48 (39-59)	47 (38 -60)	44 (35-56)	59 (42-77)	54 (46-79)
E/e	13 (10-18)	13 (10-18)	13 (10-17)	13 (9-18)	15 (11-19)	19 (15-24)	19 (13-29)
LVOTO	290 (28.9)	235 (29.0)	31 (27.9)	24 (27.6)	205 (15.4)	55 (49.1)	26 (59.1)
Significant (30≤ to <50 mm Hg)	98 (9.7)	73 (9.0)	13 (11.7)	12 (13.8)	48 (3.6)	13 (11.6)	9 (20.5)
Severe (≥50 mm Hg)	192 (19.1)	162 (20.0)	18 (16.2)	12 (13.8)	157 (11.8)	42 (37.5)	17 (38.6)
SAM	110 (10.9)	97 (12.0)	6 (5.4)	7 (8.0)	163 (12.2)	43 (38.4)	21 (47.7)

IVS, Interventricular septum; *LAVI*, left atrial volume index; *LVEDD*, left ventricular end-diastolic dimension; *LVEF*, left ventricular ejection fraction. Values are given as *n* (%) or median (interquartile range).

Table 2 Comparisons of baseline characteristics according to the presence of LVOTO

	DDS			DHDS		
	No LVOTO	Significant LVOTO (30≤ to <50 mm Hg)	Severe LVOTO (≥50 mm Hg)	No LVOTO	Significant LVOTO (30≤ to <50 mm Hg)	Severe LVOTO (≥50 mm Hg)
Demographics						
No. of patients	570	53	99	471	19	83
Age, years	65 (54-74)	60 (54-72)	65 (57-73)	61 (51-70)	57 (39-67)	60 (51-69)
Gender, male	396 (69.5)	30 (56.6)	53 (53.5)	324 (68.8)	13 (68.4)	47 (56.6)
HCM type						
Apical	268 (47.0)	7 (13.2)	2 (2.0)	110 (23.4)	2 (10.5)	2 (2.4)
Septal	145 (25.4)	23 (43.4)	54 (54.5)	318 (67.5)	16 (84.2)	75 (90.4)
Diffuse or mixed	149 (26.1)	21 (39.6)	39 (39.4)	35 (7.4)	1 (5.3)	4 (4.8)
Others	8 (1.4)	2 (3.8)	4 (4.0)	8 (1.7)	0 (0.0)	2 (2.4)
Echocardiographic data						
No. of TTEs	717	98	192	1,129	48	157
LVEDD, mm	46 (43-50)	43 (40-47)	41 (38-45)	48 (44-51)	44 (42-48)	46 (43-49)
IVS, mm	14 (12-17)	17 (14-18)	17 (15-19)	18 (16-20)	20 (16-24)	19 (16-22)
LVEF, %	65 (61-68)	65 (61-69)	66 (62-70)	67 (62-73)	74 (70-76)	71 (68-76)
LAVI, mL/m^2	45 (36-56)	44 (34-52)	50 (40-67)	42 (34-55)	45 (37-50)	53 (42-67)
E/e	12 (9-16)	13 (10-17)	17 (13-25)	14 (11-18)	16 (14-24)	20 (14-28)

IVS, Interventricular septum; *LAVI*, left atrial volume index; *LVEDD*, left ventricular end-diastolic dimension; *LVEF*, left ventricular ejection fraction. Values are given as *n*%) or median (interquartile range).

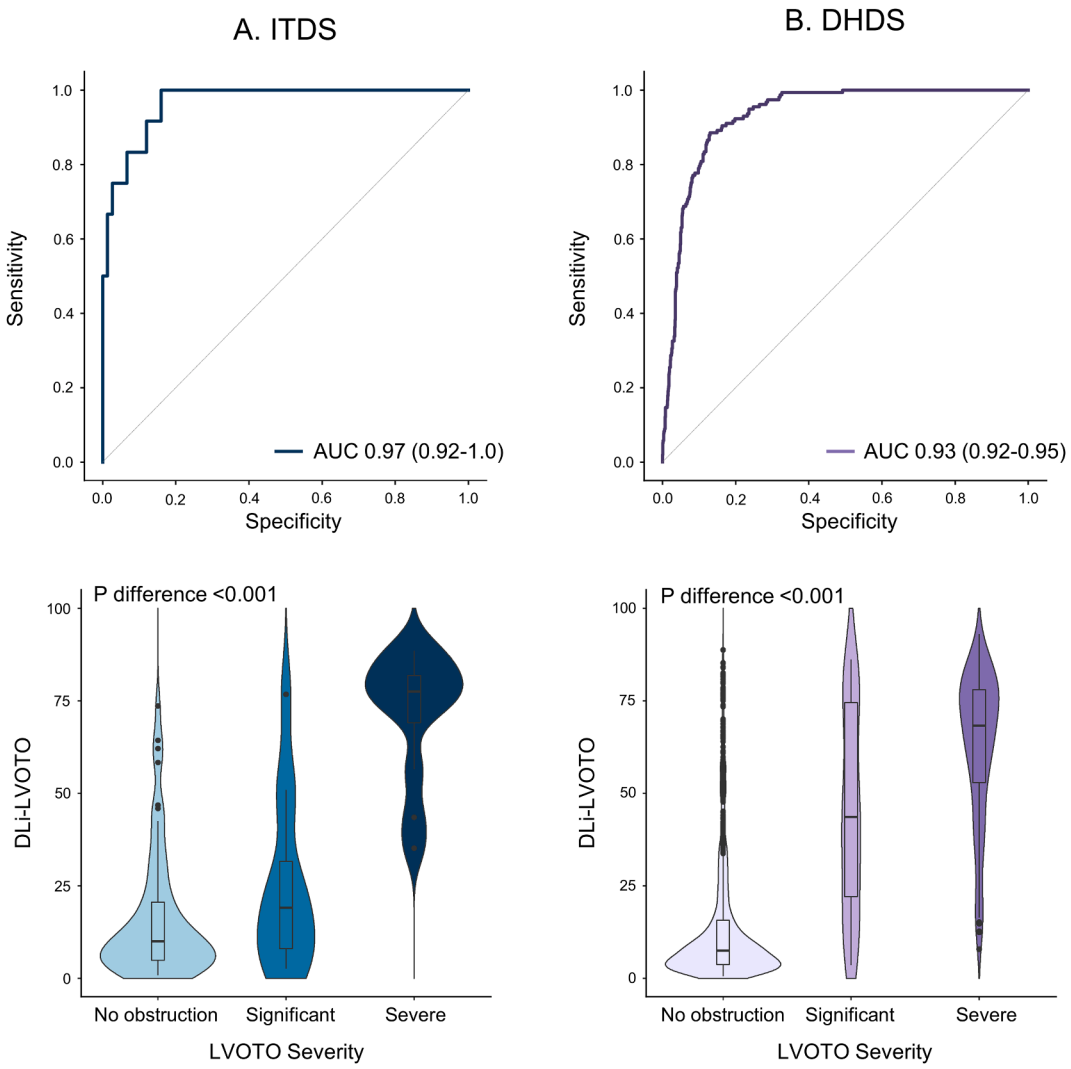

Figure 2 Model performance in the internal and external validation sets (**A**, ITDS; **B**, DHDS).

Deep learning index for LVOTO values between 30 and 70 were associated with a trade-off between sensitivity and specificity, representing an intermediate range in which additional Doppler-based assessment may be warranted for accurate classification.

For each severity level, we present representative samples with Grad-CAM saliency maps overlaid on PLAX views, specifically highlighting the LVOT region (Figure 3, Video 1). These results demonstrate that our model accurately identifies the relevant

Table 3 Diagnostic performance of DLi-LVOTO cutoffs for identifying severe LVOTO

	ITDS						DHDS					
DLi-LVOTO Cutoff	Accuracy (%)	F1-score	Sensitivity (%)	Specificity (%)	PPV (%)	NPV (%)	Accuracy (%)	F1-score	Sensitivity (%)	Specificity (%)	PPV (%)	NPV (%)
10	55.2	38.1	**100.0**	48.0	23.5	**100.0**	65.4	40.3	**99.4**	60.8	25.3	**99.9**
20	73.6	51.1	**100.0**	69.3	34.3	**100.0**	78.7	50.7	93.0	76.8	34.8	98.8
30	83.9	63.2	**100.0**	81.3	46.2	**100.0**	84.4	57.7	90.4	83.6	42.4	98.5
40	87.4	66.7	91.7	86.7	52.4	98.5	87.6	61.5	84.1	88.1	48.5	97.6
50	90.8	71.4	83.3	92.0	62.5	97.2	89.5	63.5	77.7	91.1	53.7	96.8
60	92.0	72.0	75.0	94.7	69.2	95.9	**91.3**	**64.2**	66.2	94.6	62.3	95.5
70	**94.3**	**78.3**	75.0	97.3	81.8	96.1	90.5	53.1	45.9	96.4	**63.2**	93.0
80	92.0	58.8	41.7	**100.0**	**100.0**	91.5	89.1	29.8	19.7	**98.3**	60.8	90.2

The data given in bold text is to emphasize the corresponding content in the article.

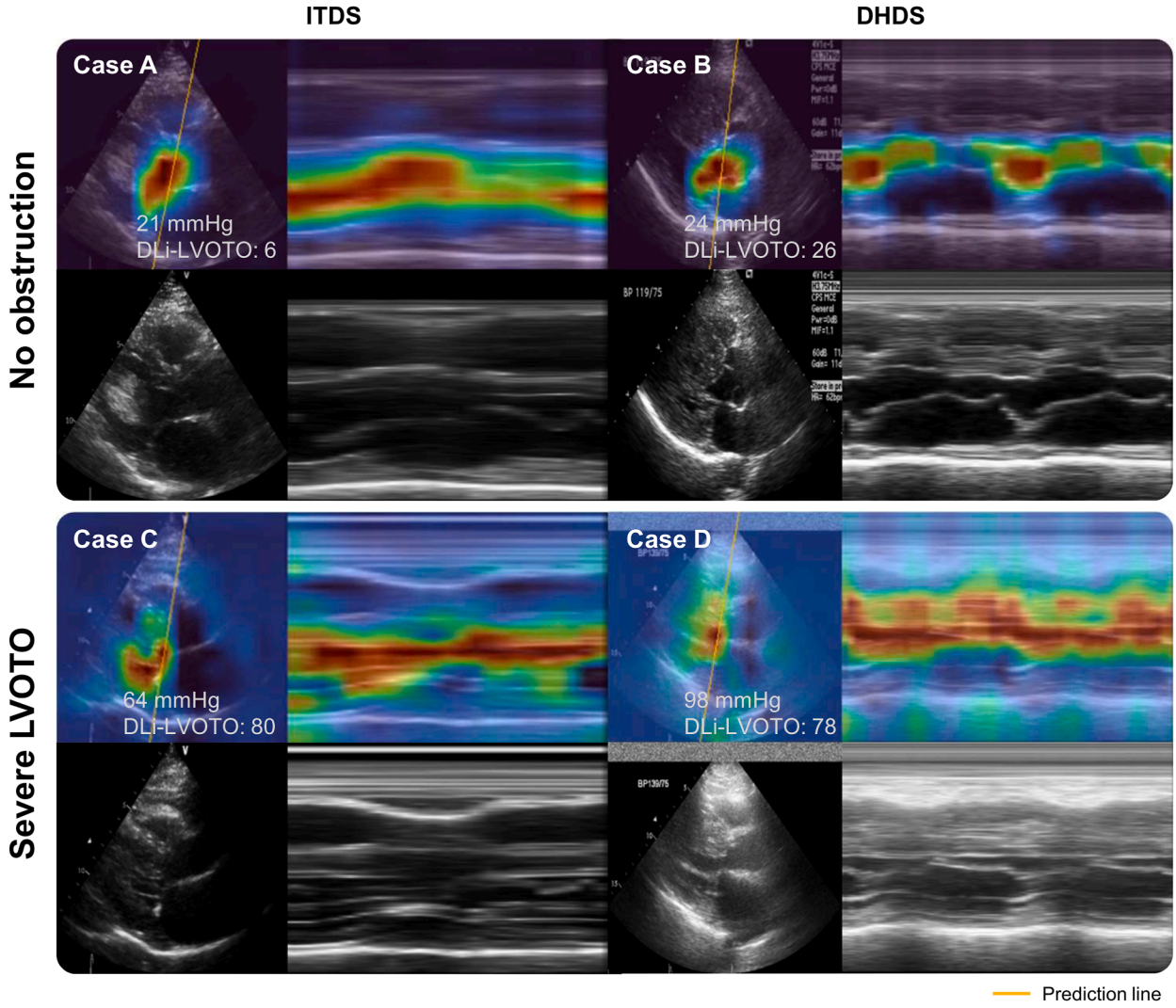

Figure 3 Explainability analysis for DLi-LVOTO using saliency map.

regions for evaluating LVOTO across all severity levels without supervision.

DLi-LVOTO Changes After LVOT Gradient Reduction Treatment

In patients who underwent LVOT gradient reduction treatment, we visualized the changes in LVOT peak PG and DLi-LVOTO between baseline and follow-up TTE exams (Figure 4). In patients who underwent surgical myectomy, LVOT peak PG showed a marked reduction postsurgery, accompanied by a corresponding decrease in DLi-LVOTO. Similarly, in patients treated with Mavacamten, both LVOT peak PG and DLi-LVOTO progressively decreased over the course of treatment compared to baseline. Representative cases are presented in Figure 5. In the patient who underwent surgical myectomy, a significant reduction in peak PG was accompanied by a corresponding decrease in DLi-LVOTO. After a while, for the patient treated with Mavacamten, when the initial treatment response was insufficient, both peak PG and DLi-LVOTO remained elevated. However, with dose escalation, a gradual decrease in both parameters was observed. To further investigate the relationship between treatment-induced changes in peak PG and DLi-LVOTO, we visualized these changes at the individual case level (Supplemental Results 4 and 5). The results demonstrated that changes in DLi-LVOTO closely paralleled changes in LVOT peak PG following treatment.

DISCUSSION

We have developed and validated a DL-based model for predicting severe LVOTO in HCM using only a single TTE view. Despite relying solely on the PLAX view, the model demonstrated high accuracy in predicting severe LVOTO, with robust performance validated not only in the ITDS but also in independent external datasets. These findings suggest that this approach could be a reliable and efficient alternative to conventional methods. Furthermore, we observed that changes in LVOT peak PG following treatment were generally accompanied by corresponding changes in DLi-LVOTO within the same patient, suggesting the model's potential utility in reflecting treatment-related trends (Central Illustration).

The application of AI in echocardiography has advanced significantly over the past decade. Early research focused on automating manual measurements, including view classification, target structure segmentation, and quantification. However, one of the core aspects

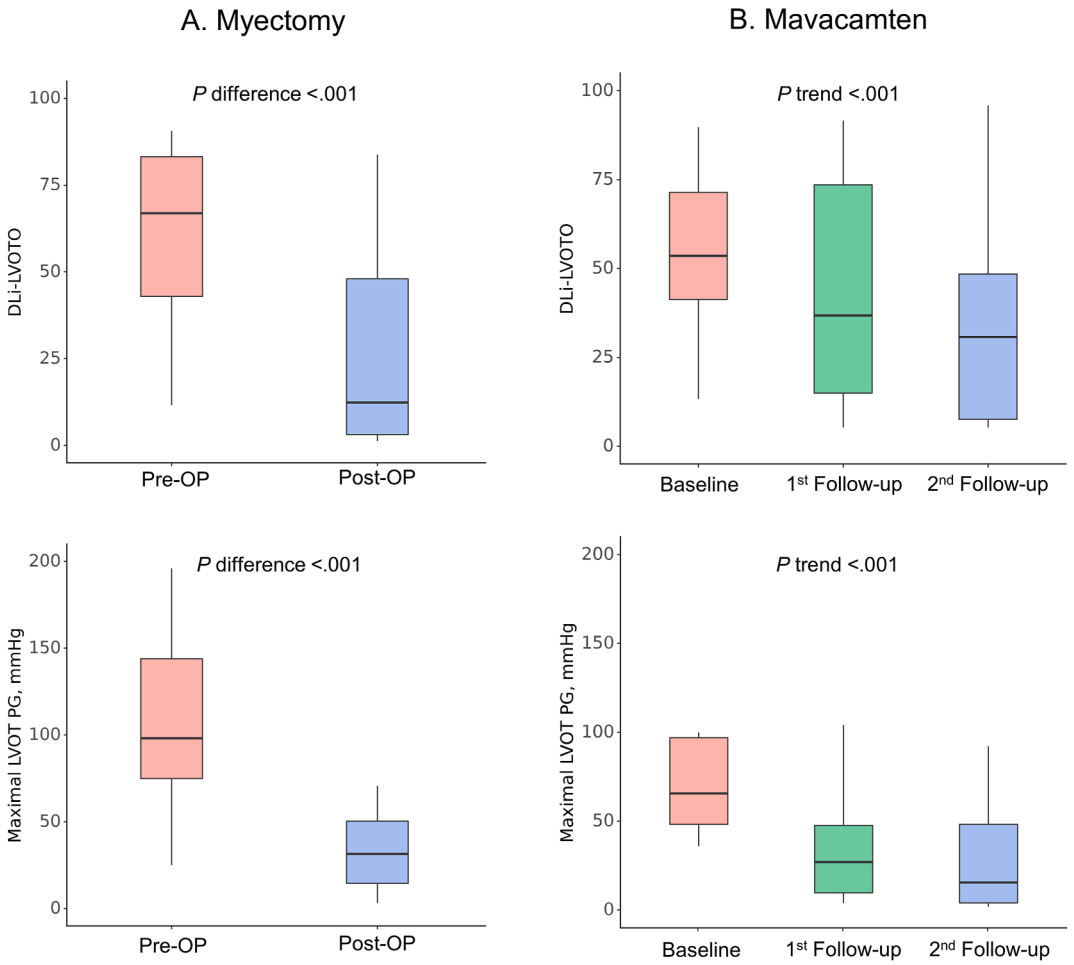

Figure 4 Interval changes in DLi-LVOTO and peak PG after LVOT gradient reduction treatment (**A**, myectomy; **B**, Mavacamten).

of echocardiographic examination—the expert-driven visual analysis—remained largely unchallenged by AI. Recent DL models have begun to mimic expert eyeball analysis, predicting diastolic dysfunction from an A4C view and AS using PLAX or parasternal short-axis views.[4-7,23] These models do not aim for a standalone definitive diagnosis but rather serve as decision-support tools, flagging potential disease and guiding further workup. Our DLi-LVOTO model extends this paradigm by enabling real-time LVOTO risk estimation during routine B-mode scanning. It has the potential to assist early decision-making in settings where Doppler assessment is not immediately available. For example, it could be integrated into handheld ultrasound devices or limited-resource environments, although further validation in such conditions would be required. Additionally, it could be integrated into handheld ultrasound devices that lack Doppler capability, allowing early detection and timely evaluation in resource-limited settings. It can also be incorporated into the standard echocardiography workflow, generating the DL-derived index during initial PLAX acquisition. This real-time feedback would prompt targeted Doppler evaluation with provocation maneuvers for high-risk cases, streamlining the diagnostic process. The DLi-LVOTO also promises longitudinal monitoring during treatment, tracking changes to evaluate the effectiveness of Mavacamten therapy or septal myectomy. To fully validate these applications, larger-scale prospective studies focusing on both the diagnostic effectiveness of DLi-LVOTO integration and treatment response tracking are warranted.

Although predicting LVOTO and AS from B-mode TTE video may be similar, key differences exist. Unlike AS, which is typically a fixed obstruction, LVOTO is inherently dynamic, fluctuating throughout the day and influenced by physiological and hemodynamic conditions. Therefore, accurate LVOTO assessment with TTE often requires provocation maneuvers, such as the Valsalva maneuver, or stress tests to induce obstruction and unmask its severity. This variability makes predicting LVOTO using only resting B-mode videos challenging. However, certain structural and hemodynamic factors that predispose patients to LVOTO development can still be evaluated on resting TTE. These include a narrowed LVOT, sigmoid septum morphology, systolic anterior motion (SAM) of the MV, and small LV cavity size, all of which contribute to flow acceleration and obstruction under specific conditions. Based on this understanding, we hypothesized that the PLAX view—a foundational TTE perspective—could serve as an optimal input for DL-based LVOTO prediction. Its clear visualization of the LVOT and key anatomical determinants of obstruction makes it particularly suited for this purpose. As a result, we successfully developed a DL-based model trained exclusively on single-view video data, capable of reliably identifying severe LVOTO, even without Doppler input or multiview analysis. This distinguishes our approach from the only existing study (preprint, not peer-reviewed) that attempted to predict LVOTO using A4C views alone.[8] We believe this difference in anatomical visualization is one of the key factors contributing to the enhanced performance observed in our study.

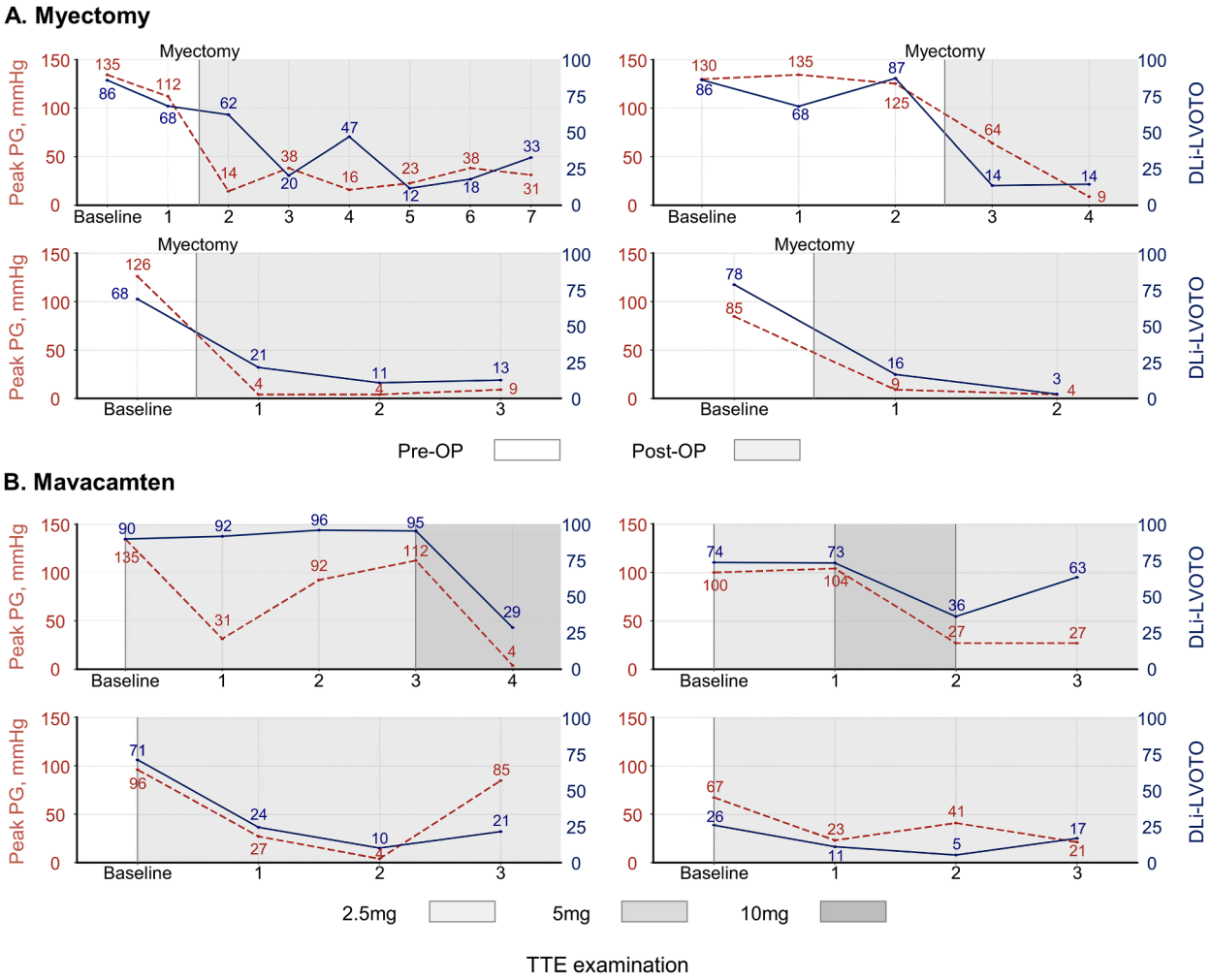

Figure 5 Representative cases for trends in DLi-LVOTO and PG with LVOT gradient reduction treatment (**A**, myectomy; **B**, Mavacamten).

Several previous studies on echocardiographic disease prediction have adopted different strategies, each with inherent limitations. For example, Huang *et al.*[23] extracted single frames from echocardiogram videos, converted them to grayscale, and resized them to 64 × 64 pixels before training a WideResNet-28 for view classification and AS diagnosis. While this 2D method is computationally efficient, its static nature makes capturing the dynamic motion patterns critical for conditions like LVOTO challenging. In contrast, Holste *et al.*[4] employed three-dimensional convolutional neural networks with extensive self-supervised pretraining and deep ensemble methods, assuming that temporal patterns would emerge implicitly from the video data. Although such approaches benefited from modeling spatiotemporal information, they did not explicitly focus on the motion of key anatomical structures and were computationally expensive. Similarly, our group previously utilized an R(2 + 1)D architecture with a continuum-aware multitask loss to accurately classify and comprehensively assess the AS continuum.[5,6,24] However, this method still relied on the network to implicitly learn temporal dynamics rather than explicitly track motion. In contrast, our current LVOTO prediction model was explicitly designed to capture both morphological and dynamic motion features crucial for LVOTO assessment. By incorporating multilevel M-mode generation and embeddings, our method enhances the detection of subtle transient motion, such as the SAM of the MV, and their resulting hemodynamic consequences. These architectural advancements contributed to the superior performance compared to a prior attempt to detect LVOTO from B-mode video only,[8] indicating its robustness and potential for clinical translation of our model.

While B-mode-derived M-mode representations have been explored in AI-driven echocardiographic analysis, the prior approach has limitations. For instance, a previous study attempted to improve cardiac function prediction by incorporating M-mode imaging for ejection fraction estimation.[25] However, their method relied on fixed sampling lines selected via heuristic rules, producing static M-mode representations that could not adapt to individual patient anatomy or dynamic motion patterns. Additionally, because M-mode extraction was performed as a separate preprocessing step, the model could not refine feature selection in an end-to-end manner, potentially limiting diagnostic performance. Our approach fundamentally differs by incorporating M-mode generation directly within the DL framework through the spatial transformer module. This allows the network to autonomously determine the most informative M-mode trajectory on a frame-by-frame basis, optimizing motion extraction as part of the training process. By jointly optimizing the trajectory selection, feature extraction, and classification, our model overcomes

the constraints of the static M-mode placement and enables more robust LVOTO detection. Furthermore, our model enhances feature extractions through multiresolution processing and bilinear fusion of B-mode and M-mode representations, providing a comprehensive understanding of both structural morphology and motion dynamics within an end-to-end framework. This integration improves classification accuracy and enhances clinical interpretability, as the network autonomously identifies and prioritizes diagnostically relevant features directly from the data. Importantly, our automated M-mode generation yields visualizations that align with traditional clinical practice, where M-mode imaging is highly valued for capturing motion over time by producing M-mode images that display critical dynamic features in a format familiar to clinicians. Moreover, Grad-CAM overlays on these generated M-mode images further enhance interpretability by highlighting the precise regions and moments of abnormal motion that drive the network's predictions.

Despite the robust performance demonstrated across internal and external datasets, it is important to recognize the trade-off between specificity and sensitivity observed at different cutoff values. As noted in our analysis, higher cutoffs increase specificity but simultaneously reduce sensitivity, potentially leading to missed severe LVOTO cases. This trade-off highlights the need for careful consideration when selecting an optimal threshold, particularly in clinical settings where the balance between false positives and false negatives must be managed according to diagnostic priorities. Unlike fixed Doppler-based criteria, our DL-based model offers the flexibility to adjust cutoff values depending on clinical context—for example, prioritizing sensitivity in initial screenings or specificity in pretreatment evaluations. Further studies are warranted to explore optimal threshold strategies tailored to specific clinical scenarios.

This study has several limitations. Although we developed and rigorously validated our DL-based model using multicenter data, including internal and external validation, all datasets were retrospectively collected from tertiary centers in South Korea. As a result, caution is required when interpreting the findings and applying them to clinical practice. Further validation across diverse populations and healthcare settings is essential to enhance generalizability. Additionally, while the DL model was evaluated using TTE data from multiple institutions, its performance in resource-limited environments or when used by novice operators remains uncertain. Whether DLi-LVOTO will perform reliably on TTE images acquired in such settings is yet to be determined. However, given that the PLAX view is one of the most fundamental TTE views and is more likely to be adequately obtained than a complete multiview TTE examination, this suggests that DLi-LVOTO could provide a reliable assessment of LVOTO in HCM patients even in less advanced settings. Second, LVOTO is not exclusive to HCM patients and can occur in various clinical settings, such as hyperdynamic states and certain cardiac structural variations. Additional studies are required to determine whether DLi-LVOTO can accurately detect LVOTO in non-HCM patients. Third, this study also examined the changes in DLi-LVOTO in response to Mavacamten or surgical myectomy treatment alongside LVOT PG, although the analysis was conducted on a relatively small patient cohort. While DLi-LVOTO generally reflected treatment-related trends, it did not always show close temporal alignment with Doppler-derived PG at every time point. This discrepancy may be attributable to physiological variability in PG or differences in what each metric captures. Further investigation is needed to evaluate the robustness and reproducibility of DLi-LVOTO as a longitudinal marker of treatment response. Lastly, future research should explore whether DLi-LVOTO can predict clinical outcomes in HCM patients. Addressing these aspects will be crucial for further validating the clinical utility of this DL-based approach.

In conclusion, our DL-based approach enables the prediction of severe LVOTO using only the PLAX view from TTE, providing a complementary tool in situations where acquiring multiple views or Doppler-based LVOT PGs is challenging. Additionally, DLi-LVOTO may support the longitudinal monitoring of treatment response by reflecting overall trends in LVOTO severity, although it is not intended to replace Doppler-based PG measurements. This method has the potential to enhance LVOTO evaluation in select clinical scenarios, supporting rather than replacing traditional assessment methods.

CONFLICTS OF INTERESTS

Y.E.Y, J.J., Y.J., J.K., and S.A.L. are currently affiliated with Ontact Health. J.J., J.K., and S.A.L are co-inventors on a patent related to this work filed by Ontact Health (Method for Providing Information for the Prediction of Left Ventricular Outflow Tract Obstruction in Hypertrophic Cardiomyopathy). H.J.C., and Y.E.Y holds stock in Ontact Health. The other authors have no conflicts of interest to declare.

SUPPLEMENTARY DATA

Supplementary data related to this article can be found at https://doi.org/10.1016/j.echo.2025.08.008.

REFERENCES

1. Maron BJ, Desai MY, Nishimura RA, et al. Diagnosis and evaluation of hypertrophic cardiomyopathy: JACC state-of-the-art review. J Am Coll Cardiol 2022;79:372-89.
2. Abbasi M, Ong KC, Newman DB, et al. Obstruction in hypertrophic cardiomyopathy: many faces. J Am Soc Echocardiogr 2024;37:613-25.
3. Wessler BS, Huang Z, Long GM Jr, et al. Automated detection of aortic stenosis using machine learning. J Am Soc Echocardiogr 2023;36:411-20.
4. Holste G, Oikonomou EK, Mortazavi BJ, et al. Severe aortic stenosis detection by deep learning applied to echocardiography. Eur Heart J 2023;44:4592-604.
5. Park J, Kim J, Jeon J, et al. Artificial intelligence-enhanced comprehensive assessment of the aortic valve stenosis continuum in echocardiography. EBioMedicine 2025;112:105560.
6. Park J, Kim J, Jeon J, et al. Deep learning-based detection and severity assessment of bicuspid aortic valve stenosis. J Am Soc Echocardiogr 2025;38:723-5.
7. Chen X, Yang F, Zhang P, et al. Artificial intelligence-Assisted left ventricular diastolic function assessment and grading: multiview versus single view. J Am Soc Echocardiogr 2023;36:1064-78.
8. Yuan V, Ieki H, Binder C, et al. Detection of left ventricular outflow obstruction from standard B-mode echocardiogram videos using deep learning. medRxiv 2025;2025.03.02.25323199. https://doi.org/10.1101/2025.03.02.25323199.
9. National Information Society Agency. Open AI dataset Project (AI-Hub). Available at: https://aihub.or.kr/. Accessed August 3, 2025.
10. Jeon J, Ha S, Yoon YE, et al. Echocardiographic view classification with integrated out-of-distribution detection for enhanced automatic echocardiographic analysis. arXiv [eess.SP; 2023]. Available at: https://arxiv.org/abs/2308.16483. Accessed August 3, 2025.
11. Jeon J, Kim J, Jang Y, et al. A Unified approach for comprehensive analysis of various Spectral and Tissue Doppler echocardiography. arXiv [eess.IV; 2023]. Available at: https://arxiv.org/abs/2311.08439. Accessed August 3, 2025.

12. Park J, Jeon J, Yoon YE, et al. Artificial intelligence-enhanced automation of left ventricular diastolic assessment: a pilot study for feasibility, diagnostic validation, and outcome prediction. Cardiovasc Diagn Ther 2024;14:352-66.
13. Jang Y, Choi H, Yoon YE, et al. An artificial intelligence-based automated echocardiographic analysis: enhancing efficiency and prognostic evaluation in patients with revascularized STEMI. Korean Circ J 2024;54:e103.
14. Ommen SR, Ho CY, Asif IM, et al. 2024 AHA/ACC/AMSSM/HRS/PACES/SCMR Guideline for the management of hypertrophic cardiomyopathy: a report of the American Heart Association/American College of Cardiology joint committee on clinical practice guidelines. Circulation 2024;149:e1239-311.
15. Tran D, Wang H, Torresani L, et al. A closer look at spatiotemporal convolutions for action recognition. In: 2018 IEEE/CVF Conference on Computer Vision and Pattern Recognition, Salt Lake City, UT, USA; 2018;. pp. 6450-9.
16. He K, Zhang X, Ren S, et al. Deep residual learning for image recognition. In: 2016 IEEE Conference on Computer Vision and Pattern Recognition, Las Vegas, NV, USA; 2016;. pp. 770-8.
17. Jaderberg M, Simonyan K, Zisserman A, et al. Spatial transformer networks. arXiv [cs.CV; 2015]. Available at: https://arxiv.org/abs/1506.02025. Accessed August 3, 2025.
18. Tan M, Le Q. EfficientNet: Rethinking model scaling for convolutional neural network. arXiv [cs.LG; 2019]. Available at: https://arxiv.org/abs/1905.11946. Accessed August 3, 2025.
19. Cubuk E, Zoph B, Shlens J, et al. RandAugment: practical automated data augmentation with a reduced search space. arXiv [cs.CV; 2019]. Available at: https://arxiv.org/abs/1909.13719. Accessed August 3, 2025.
20. Park J, Yoon YE, Jang Y, et al. Novel deep learning framework for simultaneous assessment of left ventricular Mass and longitudinal Strain: clinical feasibility and validation in patients with hypertrophic cardiomyopathy. medRxiv Available at: https://www.medrxiv.org/content/10.1101/2025.01.17.25320694v1. Accessed August 3, 2025.
21. Lang RM, Badano LP, Mor-Avi V, et al. Recommendations for cardiac chamber quantification by echocardiography in adults: an update from the American Society of Echocardiography and the European Association of Cardiovascular Imaging. J Am Soc Echocardiogr 2015;28:1-39.e14.
22. Selvaraju RR, Cogswell M, Das A, et al. Grad-CAM: visual explanations from deep networks via gradient-based localization. Int J Comput Vis 2020;128:336-59.
23. Huang Z, Long G, Wessler B, et al. A new semi-supervised learning benchmark for classifying view and diagnosing aortic stenosis from echocardiograms. Proc Mach Learn Res 2021;149:614-47.
24. Park J, Kim J, Jeon J, et al. Utilizing deep learning for accurate assessment of aortic valve stenosis: case series for clinical applications. J Cardiovasc Imaging 2025;33:3.
25. Ozkan E, Sutter TM, Hu Y, et al. M(otion)-mode based prediction of ejection fraction using echocardiograms. arXiv [eess.IV; 2023]. Available at: https://arxiv.org/abs/2309.03759. Accessed August 3, 2025.